

Simulation of vapor emissions from liquid spills

T.A. Cavanaugh II, J.H. Siegell*, K.W. Steinberg

Exxon Research and Engineering Company, 180 Park Avenue, Florham Park, NJ 07932, USA

Received 11 August 1993; accepted in revised form 18 November 1993

Abstract

An improved model for simulating vapor emissions from a multicomponent liquid spill (LSM90) has been developed incorporating three mechanisms for transfer to the gas phase: (i) flashing liquid, (ii) entrainment as aerosol, and (iii) liquid pool evaporation. The simulation accounts for both heat and mass transfer effects. Flexibility is given in describing the spill site configuration and chemical release composition. Several improvements provide a more representative simulation. Pools spread more naturally within a diked area. The pool is also checked repeatedly to determine whether vaporization is by evaporation or a boiling mechanism. Aerosol formation rates are calculated using the new AIChE CCPS RELEASE model. The DIPPR database has been incorporated to give access to the physical properties of numerous materials. The model underwent a full program of validation. A test plan using over 90 cases was designed to check: (1) trends in the model's behavior from variations in input data, and (2) the accuracy of results when compared to experimental data. Single component land spill evaporation rates were compared against experimental results reported by Kawamura, MacKay and Matsugu. The model was also tested against two sets of liquified natural gas (LNG) spills on water: Matagorda Bay and the Burro Series.

1. Introduction

Developing a plan to minimize the effects of an accidental release requires a detailed knowledge of the spill's behavior. Experimental simulation is difficult and expensive. For this reason, environmental engineers rely heavily on computer simulations to estimate release rates, model transport and diffusion of the hazardous liquids into the environment, and perform risk assessments. Recently, an improved simulation procedure for modeling the vapor emissions from liquid spills was developed.

The computer model, LSM90 (Liquid Spills Model 1990), draws upon the detailed studies in evaporation, aerosol formation, pool spreading, and heat transfer done by

* Corresponding author.

universities, laboratories, and industry. The result is a coherent procedure that simulates the entire process of liquid being discharged from a vessel, forming a pool on the ground (or a slick on water), and then evaporating.

Careful consideration was given to selecting the equations and calculation procedures used in the model. Selections were based on their applicability to a variety of spill scenarios, yet being detailed enough to capture important nuances, on being mathematically stable, not overworking inconsequential physical phenomena, and requiring easily accessible data as input.

The model is capable of handling spills which are single or multicomponent, boiling or non-boiling, land-based or water-based, and uncontained or diked. Some common applications involve assessing a pure component spill like chlorine (commonly used in water treating systems) or a multicomponent spill like gasoline. The model can also be applied to more novel applications such as assessing the mitigation effectiveness from diking (e.g. vaporization control from ammonia or LNG/LPG spills). Assessing liquid spills is important as regulations which require community worker right to know and emergency planning become more pervasive. These analyses require predictive tools which can realistically estimate evaporation rates, providing a critical input to the dispersion models currently being used to assess downwind impacts.

1.1. Special features of LSM90

Foremost among the many special features of LSM90 is the ability to model multicomponent spills. The problems posed by multicomponent spills have been overcome by several means. An accurate accounting of component inventory is kept at all times and overall mixture behavior is governed by representative properties. Vaporization checks are performed repeatedly to distinguish liquid and vapor phase compositions at each calculation step. Temperature dependent properties are treated as such.

Another limitation overcome by LSM90 is its ability to simulate both boiling and non-boiling pools. Not only will LSM90 accurately represent these pool types, it also continually adjusts for any boiling/non-boiling transitions that may occur during the simulation. This is accomplished by checking the partial pressure of the evaporating pool during each time iteration to determine if the boiling or non-boiling mechanism should be used. This feature is unique among liquid spill models.

The model also contains an advanced method for determining the pool surface area used in heat transfer and how to dynamically adjust the time step for maximum simulation speed with minimum loss of accuracy.

Finally, LSM90 resolves the problems of predicting aerosol generation rates, providing chemical property data, and passing its results to an air dispersion model, by integrating with three separate packages. These packages are discussed later.

1.2. Site configuration

The first step in performing a spill simulation is to choose a model that can be configured to closely resemble the spill scenario. This consists of the physical site

layout, the storage and leak conditions, the properties of the component being spilled, and the meteorological conditions.

The spill site is described by three items: the storage tank, the presence of a containment dike, and the composition of the spill surface. The storage tank is modeled as a vertical cylinder. It is specified by its radius and height. The tank has the option of being pressurized. A containment dike may or may not be present. If the dike exists it is assumed to be circular and is specified by radius and height. For spills on water, the dike represents a boom.

The spill surface can be either land or water. The land composition can be further classified as dry sand, wet sand, concrete, insulated concrete, or steel. The model assumes a level surface and does not allow any of the liquid to be absorbed into the ground. Water-based spills are only valid for materials which are less dense than water. These spills will be modeled as if they occurred on an open stretch of fresh water. Wave action and currents are not taken into account.

1.3. Spill components

To simplify the process of allowing any liquid to be modeled, four major assumptions governing the behavior of the liquids have been made: (1) all liquids and vapors are assumed to be ideal; (2) when a single value is needed to represent a mixture property (e.g. overall pool density), properties will be averaged; (3) all liquids are non-reacting with the surroundings and multicomponent mixtures are internally non-reactive and (4) multicomponent spills always remain well mixed.

The results will be less accurate for spills of highly viscous liquids since the size of the spreading pool cannot be accurately predicted.

1.4. Integration with other systems

LSM90 takes advantage of technology offered by three other software systems. These systems are used to provide a database of chemical properties (DIPPR), an aerosol prediction method (RELEASE), and an air dispersion model (SLAB).

The DIPPR database is used for its chemical property information. This database was developed for the AIChE and contains over 1200 chemicals. In addition to constant properties (e.g. molecular weight), equation coefficients are given for properties (e.g. liquid density) which allow them to vary during a simulation as a function of temperature.

The RELEASE model is the result of a discreet aerosol research program completed in 1989 for the AIChE Center for Chemical Process Safety [2]. LSM90 uses RELEASE solely to supply a value for fraction of unflashed liquid that forms an aerosol. The limitations of the RELEASE model, however, restrict its use to single component cases. Since the RELEASE research is on-going, the model has not yet been generally made available to the public.

SLAB is an atmospheric dispersion computer model for heavier than air releases [3]. The version incorporated with LSM90 was developed at Lawrence Livermore

Laboratories in 1990. LSM90 creates a SLAB input file which allows for direct sequential runs of the two programs.

2. Theoretical basis

The success of the simulation is based on solving simultaneous mass and heat balances around the storage tank and liquid pool. An effective computer simulation was achieved by breaking the differential equations into discrete time steps. The size of the time steps was then continually adjusted to minimize calculation errors without over-sacrificing execution speed. Table 1 is a summary of the key assumptions and simplifications used in LSM90.

2.1. Mass balance around the tank

The simulation begins at the storage vessel, where the spill rate and the resultant phases (flashed vapor, aerosol droplets, and liquid amounts) of the spill are determined. Figure 1 shows a pictorial representation of liquid discharging from a tank and being released into the environment. The spill rate is a major input to determining the size of the liquid pool. It can be approached by two methods. If the material is discharged without hindrance, then a simple Bernoulli equation is sufficient to

Table 1
Summary of key assumptions

Vertical cylindrical storage tank
Circular containment dike
Level spill surface
Spill not absorbed by ground
Spill floats on water
Spills on fresh water only
No wave action or water currents
Uniform pool thickness
Liquid and vapors behave ideally for single and multicomponents
Perfect fractionation and no superheating
Properties can be averaged
No chemical or physical reactions
Multicomponent spills are well mixed
Heuristic rules for multicomponent aerosol predictions
Pool size predicts circular pool
Circular pools can be reshaped to get heat transfer contact areas
Dike, ground, and tank temperatures remain constant but heat fluxes dampen with time
In a non-boiling pool, the composition of the air above the pool does not change significantly
Total mass in pool is constant during a discrete time step
Pool temperature is constant during a discrete time step
Maximum allowable change in pool mass per time step is 1%
Maximum allowable change in pool temperature per time step is 1 K

determine the rate:

$$\text{rate} = c_D \rho A_{\text{hole}} \sqrt{2g \left[\frac{(P_{\text{stor}} - P_{\text{amb}})}{\rho g} + (h_{\text{tank}} - h_{\text{hole}}) \right]} \quad (1)$$

However, some materials may flash so readily upon release that the vapor expansion in front (or inside) the hole can actually slow the rate. In this case, the 2-phase choked flow equation of Fauske-Epstein should be used:

$$\text{rate} = c_D A_{\text{hole}} \sqrt{2\rho (P_{\text{stag}} - P_{\text{sat}}) + \frac{\Delta H_{\text{vap}}^2}{2\Delta V^2 T C_p}} \quad (2)$$

Once the spill rate is known, the amount of material flashing and forming an aerosol are subtracted to determine the amount of liquid available to form a pool.

2.2. Release mechanisms

As the liquid leaves the vessel it may immediately flash, become entrained as aerosol droplets, or fall as a liquid on the surface to form a pool. LSM90 will automatically calculate the fraction flashing. Flashing occurs when the storage temperature is greater than the normal boiling point. The mass fraction of the liquid flashed to a vapor is found by performing an isenthalpic energy balance from the storage temperature to the normal boiling point of the liquid.

$$M_{\text{flash}} = M_{\text{total}} f_{\text{flash}} \quad (3)$$

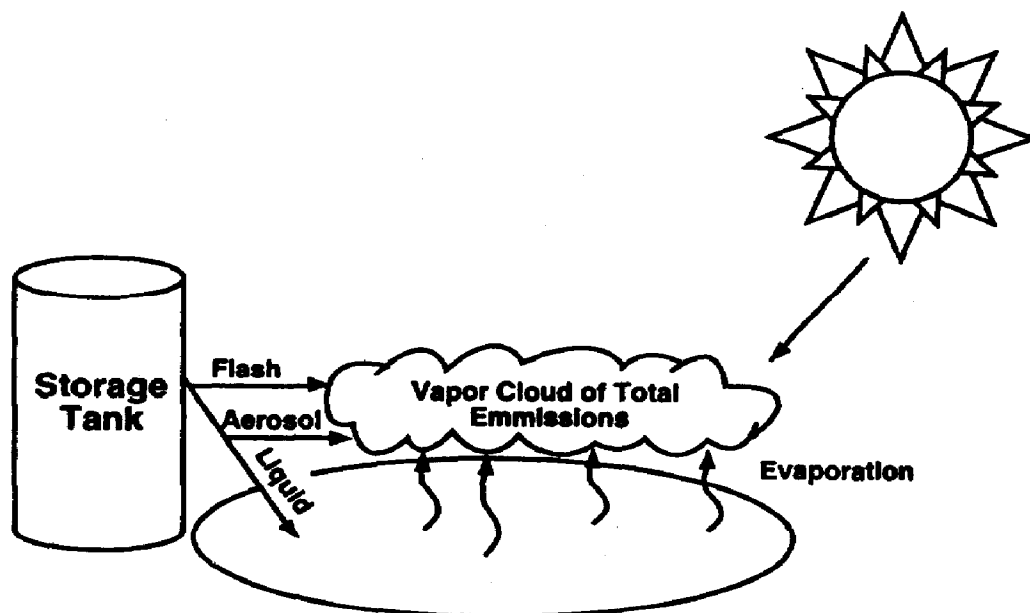


Fig. 1. Liquid discharging from a tank and being released into the environment.

Aerosoling may occur for two reasons. The discharge of the liquid may be forceful enough to atomize the liquid into aerosol droplets. Alternatively, if the flashing is particularly violent, the vapors may entrain the liquid as droplets. The aerosol fraction is defined to be a fraction of the unflashed liquid, not a fraction of the total liquid being released. The AICHE RELEASE model is used to calculate the aerosol fraction for single component releases.

For multicomponent releases the aerosol fraction is calculated using the following heuristic rules based on the temperature difference between the liquid in the storage tank and its normal boiling point. Note that Eq. (6), a linear interpolation between Eqs. (4) and (5), is used to provide a smooth transition.

$$\text{If } T_{\text{storage}} > T_{\text{nbp}} + 10, \text{ then } f_{\text{aerosol}} = 1.0 \quad (4)$$

$$\text{If } T_{\text{storage}} < T_{\text{nbp}}, \text{ then } f_{\text{aerosol}} = 0.0 \quad (5)$$

$$\text{If } T_{\text{nbp}} < T_{\text{storage}} < T_{\text{nbp}} + 10, \text{ then } f_{\text{aerosol}} = (T_{\text{storage}} - T_{\text{nbp}})/10. \quad (6)$$

Once the aerosol fraction is known, the amount forming an aerosol is given by

$$M_{\text{aerosol}} = (M_{\text{total}} - M_{\text{flash}})f_{\text{aerosol}}. \quad (7)$$

The total mass balance around the storage tank is stated as

$$M_{\text{total}} = M_{\text{flash}} + M_{\text{aerosol}} + M_{\text{to pool}}. \quad (8)$$

The liquid mass actually going to the pool is found by rearranging Eq. (8) to give

$$M_{\text{to pool}} = M_{\text{total}} - M_{\text{flash}} - M_{\text{aerosol}}. \quad (9)$$

2.3. Pool size

The released material that does not flash or become entrained as an aerosol will form a pool on the surface. The size of the pool depends on the release rate from the tank and the evaporation rate. After the release has stopped the pool will continue to evaporate and shrink in size. When the pool disappears (dries up) and the spill rate has ceased, the simulation will stop.

Equations governing the spread of a vaporizing pool can be found in the document "Evaporation from Spills of Hazardous Liquids on Land and Water" by P. Shaw and F. Briscoe [4]. These equations predict the pool radius as a function of time for circular pools of a uniform thickness. Since a spreading pool is really thinner at its edges, the equations below have been modified to use a triangular cross section instead of a rectangular one. The choice of which of the two equations should be used is based on the amount of liquid still spilling into the pool. For a pool that is still gaining mass use

$$r_{\text{new}}^2 = r_{\text{old}}^2 + \frac{4}{3} \sqrt{\frac{2gB}{\pi}} \Delta t \left[\frac{\Delta V_{\text{new}}^{1.5} - \Delta V_{\text{old}}^{1.5}}{\Delta V} \right]. \quad (10)$$

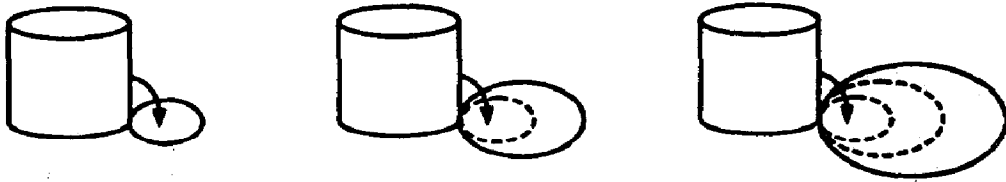


Fig. 2. Uncontained pool spreading.

When the flow to the pool has stopped, the pool continues to spread as if it were an instantaneous spill. In this situation, the radius may be found by

$$r_{\text{new}}^2 = r_{\text{old}}^2 + \frac{4}{3} \sqrt{\frac{2gB}{\pi}} \Delta t \sqrt{\Delta V_{\text{new}}} \quad (11)$$

It should be noted that both Eqs. (10) and (11) ignore any viscosity and surface tension effect and assume that the spread of the pool is due to the conversion of gravitational potential energy into kinetic energy. Therefore, these equations may not be valid for highly viscous materials. For spills onto water, the buoyancy factor, B , can be calculated as the difference in density between the water and the material divided by the density of the water. For land spills, the buoyancy factor equals 1.0. Once the radius and volume are known, other dimensions such as height and surface area can easily be calculated.

2.4. Pool shape

When calculating the size of the pool, Eqs. (10) and (11) give the radius for a circular shaped pool. Although this may not be the best physical representation for the shape of the pool, the equations do allow a surface area to be calculated. LSM90 goes one step further. It uses this surface area but then reshapes the pool to more closely resemble an actual spill. This is especially important when it comes to establishing contact areas for heat transfer with the spill surface, tank, and dike.

Figure 2 shows a pool spreading at a spill site which does not have a containment dike. In this case, the pool is assumed to expand as a circle. It will not have any surface contact with the tank.

Figure 3 is more complex. It shows how an expanding pool is reshaped at a spill site that has a containment dike. At first the pool will behave as if no dike were present, i.e. it would expand as a circle without making contact with the tank. However, once the pool reaches the dike it can no longer grow radially. At this point the pool area is reshaped into a wedge with an imaginary vertex at the center of the tank. This gives two contact areas, one with the tank and the other with the dike. As the pool continues to grow, the wedge will expand laterally to fill the area between the tank and the dike. When the tank is completely surrounded, any additional growth will cause the level of the pool to rise. A decreasing pool (one that is drying faster than it expands) will retain its present shape and area until a minimum pool thickness is reached. From then on, any further departure of mass will reduce the pool's radius.

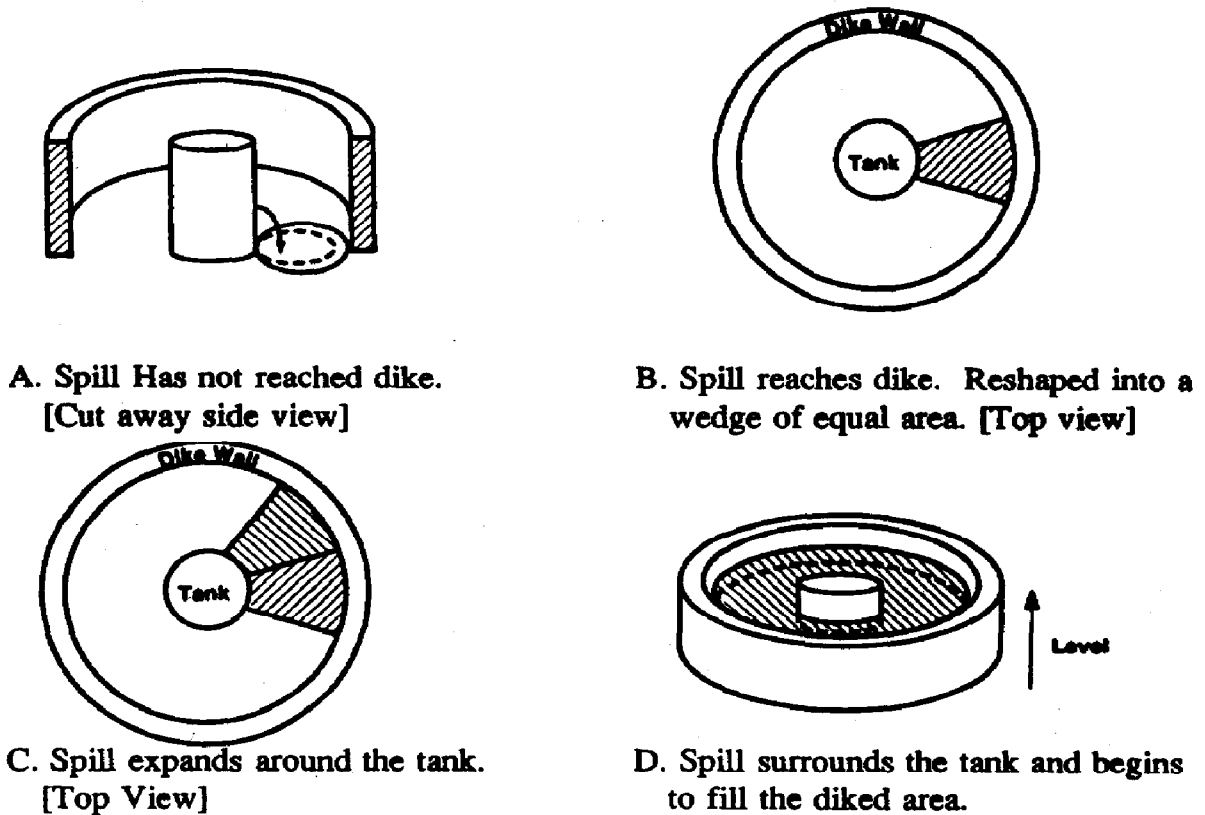


Fig. 3. Pool spreading within a containment dike.

2.5. Heat transfer

Energy may enter or leave the pool from a number of sources by means of conduction, convection, radiation and evaporation. In addition, the pool may accumulate or lose energy in the form of sensible heat. The net result, though, will be for the pool to be in balance as described by

$$q_{\text{air}} + q_{\text{dike}} - q_{\text{evap}} + q_{\text{ground}} + q_{\text{mass_add}} + q_{\text{rad}} + q_{\text{sensible}} + q_{\text{sun}} + q_{\text{tank}} = 0. \quad (12)$$

Heat of convection

The rate of convective heat transfer from air to the pool can be expressed simply as

$$q_{\text{air}} = hA(T_{\text{amb}} - T_{\text{pool}}). \quad (13)$$

The difficulty in using the above equation lies in providing a value for the heat transfer coefficient, h . Data on convective heat transfer from the atmosphere to large bodies of water are very limited. The correlations that do exist are usually expressed in the j -factor form, stressing the analogy between heat and mass transfer.

On the other hand, an empirical relation for the heat flux due to convection was derived from heat and mass transfer theory and from experimental correlations. This

relation is used in LSM90 and is expressed as

$$q_{\text{air}} = 0.004 u_w^{0.78} (2R_{\text{pool}})^{-0.11} \rho_m C_{\text{pm}} Pr^{-0.67} (T_{\text{amb}} - T_{\text{pool}}) A. \quad (14)$$

Heat from dike walls

The rate of heat transferred by contact with the walls of a containment dike is

$$q_{\text{dike}} = \sum_{i=0}^N \frac{[2k(T_{\text{dike}} - T_{\text{pool}}) A_i]}{\sqrt{\pi\alpha}(\sqrt{t} - \sqrt{t_i^*})}. \quad (15)$$

The model uses a constant uniform dike temperature throughout the simulation. In reality, the dike and pool will approach the same temperature where they meet. To simulate this the total contact area is divided into separate sections based on the time each section first came in contact with the expanding pool. The term $(\sqrt{t} - \sqrt{t_i^*})$ appears in the denominator. As the simulation progresses, the current time, t , will increase while t_i^* remains fixed. Thus, the term will become larger and cause the rate of heat transferred from that section to decrease. This technique is also applied in calculating q_{ground} and q_{tank} .

Heat loss from evaporation

The heat lost by the pool due to evaporation is simply the sum of each evaporating component times its heat of vaporization.

$$q_{\text{evap}} = \sum_{j=1}^M m_j \Delta H_{\text{vap},j}. \quad (16)$$

Heat from ground conduction

The rate of heat transferred by conduction through the ground is analogous to Eq. (15) and given as

$$q_{\text{ground}} = \sum_{i=0}^N \frac{[2k(T_{\text{ground}} - T_{\text{pool}}) A_i]}{\sqrt{\pi\alpha}(\sqrt{t} - \sqrt{t_i^*})}. \quad (17)$$

Heat of material added

If the material is still spilling from the vessel, heat will also enter the pool from the addition of the new liquid.

$$q_{\text{mass_add}} = m_{\text{to pool}} C_p (T_{\text{storage}} - T_{\text{pool}}). \quad (18)$$

Radiative heat transfer

The heat transferred from the atmosphere is known as long wave radiation. The heat emitting (or radiating) propensity of a surface is referred to as its emissivity. Depending on the direction of heat flow the pool will either be absorbing long wave radiation from the atmosphere or emitting it back. The radiation equation is expressed as

$$q_{\text{rad}} = \sigma \varepsilon f_{\text{area}} (T_{\text{amb}}^4 - T_{\text{pool}}^4) A. \quad (19)$$

Sensible heat

The sensible heat in the system is measured by the change in the pool's temperature and represents the accumulation term in a general heat balance. For the most part, this is the heat that brings everything in balance. For example, if the sum of the other heats is greater than zero, it means that more energy is entering the pool than leaving. To maintain a balance, the sensible heat would show a rise in the pool temperature. Conversely, a net negative heat would cause the pool to cool down. Of course the pool temperature can never exceed its boiling point, so in this case any extra heat is lost by additional evaporation. The sensible heat is expressed as

$$q_{\text{sensible}} = \frac{m_{\text{pool}} C_p (T_f - T_i)}{\Delta t} \quad (20)$$

Short wave radiation

The radiation from the sun is known as short wave radiation because it refers to the short wavelength of the visible spectrum. By considering the daily sun cycle as a sine wave, the heat transferred from the sun can be written in terms of the peak (noon) radiation on a clear day:

$$q_{\text{sun}} = (1 - F_r) S_{\text{noon}} \sin \left(\frac{\pi(t_D - SR)}{h_D} \right) (1 - cc) A. \quad (21)$$

This equation has the advantage of accounting for the spill hour and the subsequent passage of time. Obviously, q_{sun} at night is equal to zero.

Heat from storage tank

The rate of heat transferred by conduction through the storage tank is expressed by the same equation used for q_{dike} and q_{ground} . It is used when the liquid spill makes contact with the tank as shown in Fig. 3. It is

$$q_{\text{tank}} = \sum_{i=0}^N \frac{[2k(T_{\text{tank}} - T_{\text{pool}}) A_i]}{\sqrt{\pi\alpha}(\sqrt{t} - \sqrt{t_i^*})} \quad (22)$$

2.6. Mass evaporation

The calculation of evaporation rates for single and multicomponent spills is one of the primary objectives for LSM90. There are two methods of calculation, one for boiling pools and one for non-boiling pools. To perform an effective simulation, the status of the pool should be tested repeatedly. Each time it is determined whether the pool is boiling or non-boiling, the appropriate calculation procedure can be used.

A pool will boil if its total partial pressure is greater than the ambient pressure. To calculate the boiling rate, a heat balance must first be done around the pool using Eq. (11) to solve for q_{evap} . If q_{evap} is negative then the pool has excess energy which must be removed by boiling. A standard flash calculation will show how much mass must be boiled to remove the necessary amount of energy. If q_{evap} was positive then the pool has lost the energy it needed to maintain boiling. This will cause the pool to

stop boiling and perhaps even lower its temperature. At this point, the material in the pool will continue to evaporate, but will do so as a non-boiling pool.

The calculation of evaporation rates for non-boiling pools is based on conventional convective mass transfer theory. The evaporation equation is expressed as

$$\frac{dN_i}{dt} = - \frac{K_{gi} A N_i p_i^s}{N_T} \quad (23)$$

The mass transfer coefficient is an empirical value that solves a steady-state atmospheric diffusion equation with power-law vertical velocity and eddy diffusivity profiles based on the work of Sutton [5]. The transfer coefficient can be found using

$$K_{gi} = \frac{0.0292 u_w^{0.76} d_0^{-0.11} Sc_i^{-0.67}}{RT_{\text{pool}}} \quad (24)$$

The Schmidt number is a function of the diffusivity of the component in air. The diffusivity can be calculated using the Wilke and Lee method [6]. LSM90 assumes that the component is always diffusing into pure air. In other words, there is no build up of concentration in cloud due to previous evaporation. This greatly simplifies the calculation procedure by eliminating the need to calculate representative properties for an air-component vapor cloud. It also eliminates the need for calculating cloud concentration gradients as the vapor is carried from the pool surface by the wind. More importantly, this assumption tends to overpredict the evaporation rate, thus giving a worst-case approach to this aspect of the simulation. When using the equation, the Schmidt number should be calculated at pool temperature.

2.7. Time steps

Simulating the vaporization of a liquid spill over time can be accomplished by calculating the state of the system using successive time steps. When choosing a size for the time step, two objectives must be met: the calculations must not lose accuracy (this tends to favor a small step size) and the simulation must be completed in a reasonable amount of time (this favors a large step size). The trick is to choose a size that satisfies both objectives.

LSM90 has taken the variable time step approach. This means that the step size will continually be adjusted during the simulation based on some simple rules. If accuracy is being lost, then the calculations will be redone using a smaller step. If accuracy is being exceeded, then the time step will be lengthened for the next set of calculations.

Many of the heat and mass balance equations assume that some of the continuously changing parameters can be considered constant during each time step. Two of these parameters are the total mass of the pool and the pool temperature. By selecting some maximum allowable values for change, a standard for measuring accuracy can be established. For example, impose that the mass in the pool should never change more than 1% in any given time step and the temperature change should always be less than 1 K. If either of these conditions are violated a shorter time step is calculated and the calculations are redone. On the other hand, if both conditions are satisfied, then

attempt to lengthen the step by first extrapolating how large the step could have been and then backing off by 25%. The 25% backoff is used to prevent the simulation from pushing against the absolute maximum step.

3. The computer program

The LSM90 model was developed for delivery on an IBM compatible personal computer operating under DOS 3.2. It requires an 80287 math coprocessor and 640 K

Table 2
Input to LSM90

General information	Flash rate
Case description	Auto flash calc. [Y/N]
Engineer name	Flash fraction
Output filename	
Print rate files [Y/N]	Storage conditions
Rates filename	Storage temperature
Print composition files [Y/N]	Tank initial fluid height
Pool composition filename	Hole height
Cloud composition filename	Aerosol formation
Property database filename	Auto aerosol calc. [Y/N]
Max. simulation time	Aerosol fraction
Min. film thickness (mm)	Storage pressure
Dispersion model	Hole diameter
	Slip ratio
Spill surface	Relative humidity
Ground composition	Axial position
Ground temperature	Weber number
	N density
Site configuration	Bubble factor
Dike present [Y/N]	Entrainment constant
Dike composition	Spread angle
Dike height (m)	Expansion flag
Dike radius (m)	Liquid coefficient
Tank radius	Homogeneous coefficient
	Subcooled coefficient
Release rate	Atmospheric conditions
Spillrate calc. option number	Ambient temperature
Calc'd spill rate c_D	Ambient pressure
Spill duration auto	Wind speed
Constant spill rate1	Cloud cover fraction
Constant spill rate2	Initial hour of spill
Constant spill rate3	Sunrise time
Constant spill rate4	Sunset time
Constant spill rate5	
Spill rate duration1	Spill components
Spill rate duration2	Number of components
Spill rate duration3	Component name
Spill rate duration4	Component mass fraction
Spill rate duration5	

```

'LSM90 START'
'Case description (40 char) : ' Demo case for LSM90 presentation '
'Engineer name (40 char) : ' T. Cavanaugh

'Output filename (40 char) : ' democase.out
'Print Rates file (1=YES,0=NO) : ' 1
'Rates Filename (40 char) : ' democase.rat'
'Print Comp files (1=YES,0=NO) : ' 1
'PoolComp filename (40 char) : ' democase.po'
'CloudComp filename (40 char) : ' democase.co'
'Database filename (40 char) : ' dipper.dat'

'Max Simulation Time (sec) : ' 999999

'Ground Composition (0-6) : ' 6
'Ground Temperature (K) : ' 293.15

'Dike Present (1=YES,0=NO) : ' 1
'Dike Composition (1-7) : ' 6
'Dike Height (m) : ' 0.102
'Dike Radius (m) : ' 0.227

'Min Film Thickness (mm) : ' 11.11

'Spillrate calc (0=user;1=ch;2=b) : ' 0
'Calcd Spill rate CD : ' 1.00
'Spill Duration Auto : ' 7200
'Const spill rate1 (m3/sec) : ' 0.007
'Const spill rate2 (m3/sec) : ' 0
'Const spill rate3 (m3/sec) : ' 0
'Const spill rate4 (m3/sec) : ' 0
'Const spill rate5 (m3/sec) : ' 0
'Spill rate duration1 (sec) : ' 1
'Spill rate duration2 (sec) : ' 0
'Spill rate duration3 (sec) : ' 0
'Spill rate duration4 (sec) : ' 0
'Spill rate duration5 (sec) : ' 0

'Auto Flash Calc (1=YES,0=NO) : ' 1
'Flash Fraction (0.0 - 1.0) : ' 0.0
'Auto Aerosol Calc (1=YES,0=NO) : ' 0
'Aerosol Fraction (0.0 - 1.0) : ' 0.0

'Slip ratio (def=1) : ' 1.0
'Relative humidity (%) : ' 63.0
'Axial position (def=10) : ' 10.0
'Weber number (def=10) : ' 10.0
'N density (def=10e10/m3) : ' 10e10
'Bubble factor (def=1) : ' 1.0
'Entrainment constant (def=0.32) : ' 0.32
'Spread angle (def=4.46) : ' 4.46
'Expansion flag (1=YES,0=NO) : ' 0
'Liquid coefficient (def=0.6) : ' 0.6
'Homogeneous coeff (def=1.0) : ' 1.0
'Subcooled coefficient (def=0.6) : ' 0.6

'Tank Radius (m) : ' 0.001
'Tank initial fluid ht (m) : ' 10000
'Storage temperature (K) : ' 293.15
'Storage pressure (kPa.g) : ' 0.0
'Hole diameter (m) : ' 0.02
'Hole height (m) : ' 0

'Ambient temperature (K) : ' 298.
'Ambient pressure (kPa.a) : ' 101.3
'Wind speed (m/sec) : ' 4.94
'Cloud cover fraction(0.0 - 1.0) : ' 0.2
'Initial hour of spill (hr) : ' 9.25
'sunrise (military hr) : ' 6
'sunset (military hr) : ' 18

'Number of Components : ' 2
'Component Name (40 char) : ' '1-Butene'
'Component mass fraction (0-1) : ' 0.4
'Component Name (40 char) : ' 'n-Pentane'
'Component mass fraction (0-1) : ' 0.6
'Dispersion Model (8 char) : ' 'SLAB'
'LSM90 END'

```

Fig. 4. LSM90 sample input file.

of RAM. The program was written in FORTRAN 77 and the size of the executable file is 203 kilobytes. The execution time varies according to each simulation case but is typically measured in minutes. There are a possible 63 input items and 22 output items which are described below.

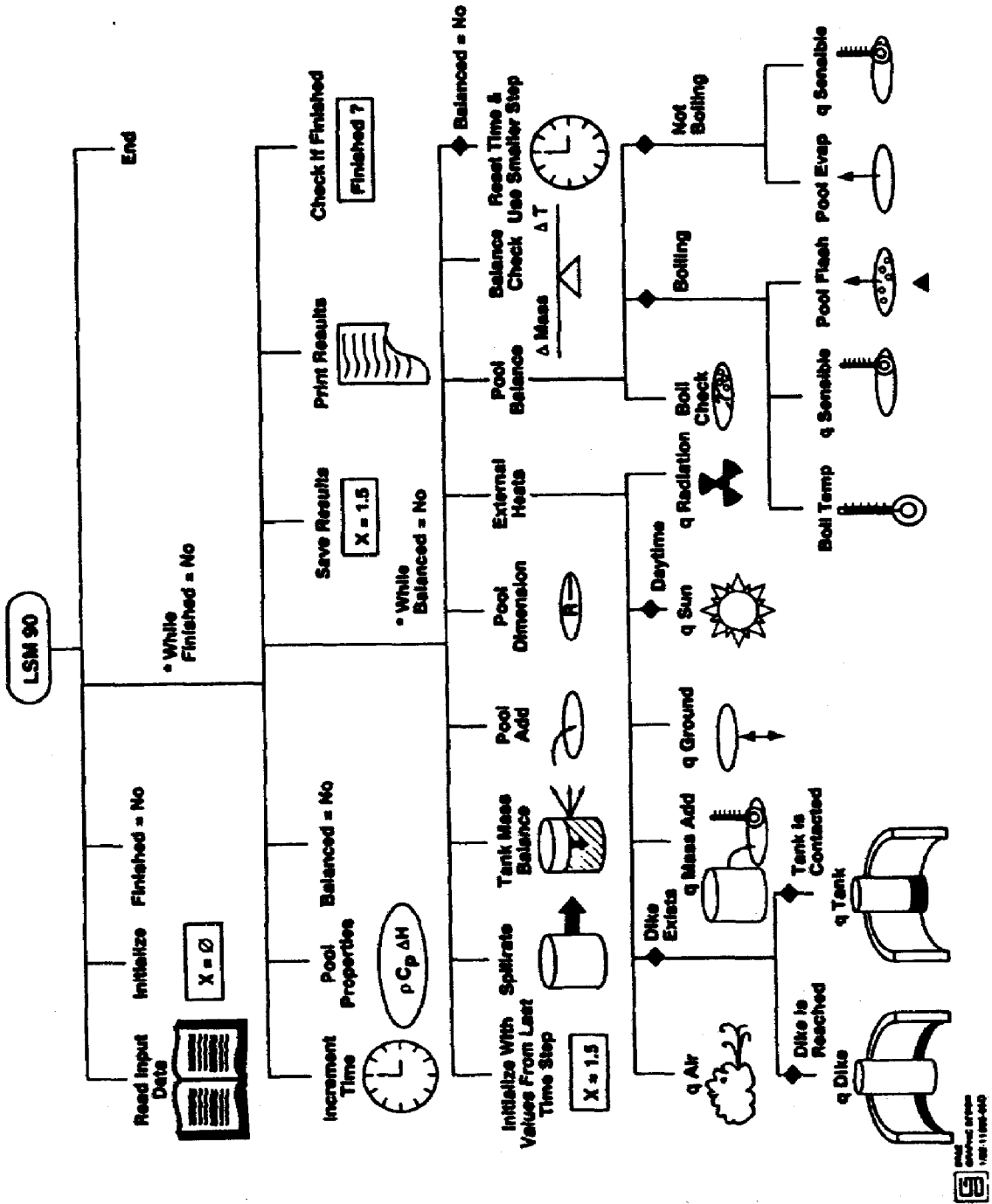


Fig. 5. Conceptual flow diagram.



3.1. Model input

Easy accessibility of input data was one of the criteria that went into selecting the equations and procedures used in LSM90. Although there are 63 possible input items, only a subset is required for any single simulation. This is because many of the items are option specific. A summary list of the items, broken down into categories, is given in Table 2 and Fig. 4 shows a sample input file.

3.2. Model execution sequence

The basic execution sequence in the program is shown by the following conceptual flow diagram, Fig. 5. This diagram illustrates the time sequencing, mass and heat balances, and convergence loops.

Table 3
LSM90 output items

Actual time simulated	Average insolation
Reason for termination	Time (hh:mm:ss)
Time average pool temperature	Total vapor rate
Average evaporation rate	Flash rate
Average specific evaporation rate	Aerosol rate
Maximum cloud rate	Evaporation rate
Time average cloud rate	Cumulative mass out
Final pool size	Mass in pool
Total amount released	Pool area
Total amount to pool	Pool temperature
Total amount left in pool	Component mole fraction

```

*****
                LIQUID SPILLS MODEL                Apr 15 1991 18:08:49
*****
Computer Model   : LSM90
Case Description: Demo case for LSM90 presentation
Engineer        : T.Cavanaugh
Output File Name: democase.out
*****

Actual time simulated (HH:MM:SS)      : 03:37:32
Reason for termination                 : Pool dried and no more spill
Time average pool temp(deg K)         : 257.44
Average evaporation rate(Kg/hr)       : .951
Average specific evap. rate(Kg/hr/sq.m) : 17.26209
Maximum cloud rate(Kg/hr)             : 3087.65
Time average cloud rate(Kg/hr)        : 1.106
Final pool size(sq.m)                 : .000
Total amount released(Kg)              : 3.682
Total amount to pool(Kg)              : 3.447
Total amount left in the pool(Kg)     : 0.000
Average insolation(Kcal/hr/sq.m)      : 402.08

```

Fig. 6. LSM90 output, part of a SUMMARY report.

```

*****
                LIQUID SPILLS MODEL                Apr 16 1991 16:44:45
*****
Computer Model : LSM90

Case Description: Demo case for LSM90 presentation
Engineer       : T. Cavanaugh
Output File Name: democase.rat
*****

```

Time HH:MM:SS	Total Vapor Rate (Kg/s)	Flash Rate (Kg/s)	Aerosol Rate (Kg/s)	Evap. Rate (Kg/s)	Cumulat Mass Out (Kg)	Mass in Pool (Kg)	Pool Area (M2)	Pool Temp (K)
00:00:00	.000	.000	.000	.000	.00	.00	.0	282.2
00:00:01	.086	.081	.000	.005	1.23	1.15	.2	281.8
00:00:02	.046	.041	.000	.005	3.07	2.87	.2	281.8
00:00:03	.046	.041	.000	.005	3.68	3.43	.2	281.7
00:00:04	.005	.000	.000	.005	3.68	3.43	.2	281.5
00:00:05	.005	.000	.000	.005	3.68	3.42	.2	281.3
00:00:06	.005	.000	.000	.005	3.68	3.42	.2	281.0
00:00:07	.005	.000	.000	.005	3.68	3.41	.2	280.8
00:00:08	.005	.000	.000	.005	3.68	3.41	.2	280.6
00:00:09	.005	.000	.000	.005	3.68	3.41	.2	280.4
00:00:10	.005	.000	.000	.005	3.68	3.40	.2	280.2
00:00:15	.005	.000	.000	.005	3.68	3.38	.2	279.1
00:00:20	.004	.000	.000	.004	3.68	3.35	.2	278.1
00:00:25	.004	.000	.000	.004	3.68	3.33	.2	277.1
00:00:30	.004	.000	.000	.004	3.68	3.31	.2	276.2
00:00:35	.004	.000	.000	.004	3.68	3.29	.2	275.3
00:00:40	.004	.000	.000	.004	3.68	3.27	.2	274.4
00:00:45	.004	.000	.000	.004	3.68	3.26	.2	273.6
00:00:50	.004	.000	.000	.004	3.68	3.24	.2	272.8

Fig. 7. LSM90 output, part of RATES report.

```

*****
                LIQUID SPILLS MODEL                Apr 16 1991 16:44:45
*****
Computer Model : LSM90
Case Description: Demo case for LSM90 presentation
Engineer       : T. Cavanaugh
Output File Name: democase.co
*****
Composition of Cloud(mole fraction)
-----

```

Time hh:mm:ss	1	2	3	4	5	6	7	8	9	10
00:00:00	.000	.000								
00:00:01	.810	.190								
00:00:02	.808	.192								
00:00:03	.808	.192								
00:00:04	.808	.192								
00:00:05	.808	.192								
00:00:06	.808	.192								
00:00:07	.808	.192								
00:00:08	.808	.192								
00:00:09	.808	.192								
00:00:10	.808	.192								
00:00:15	.807	.193								
00:00:20	.807	.193								
00:00:25	.807	.193								
00:00:30	.806	.194								
00:00:35	.806	.194								
00:00:40	.805	.195								
00:00:45	.805	.195								
00:00:50	.805	.195								

Fig. 8. LSM90 output, part of a COMPOSITION report.

3.3. Model output

The output from LSM90 can be used to predict evaporation rates, spill sizes, and pool temperatures for liquid spills. The output consists of one standard report summarizing the results and three optional reports showing (1) vapor emission rates, (2) pool composition and (3) vapor cloud compositions over time. The 22 output items available to the user are summarized in Table 3 while Figs. 6-8 show portions of the sample output files.

4. Validation

The model underwent a full program of validation. A test plan using over 90 cases was designed to check:

- (1) the trends in the model's behavior from variations in input data, and
- (2) the accuracy of results when compared to experimental data.

4.1. Tests for behavioral trends

The testing looked at the effect of various input variables. In these parametric tests, 75 parametric simulations were run to show how the evaporation rate was affected by changes in surface temperature, surface type, wind speed, ambient temperature, spill

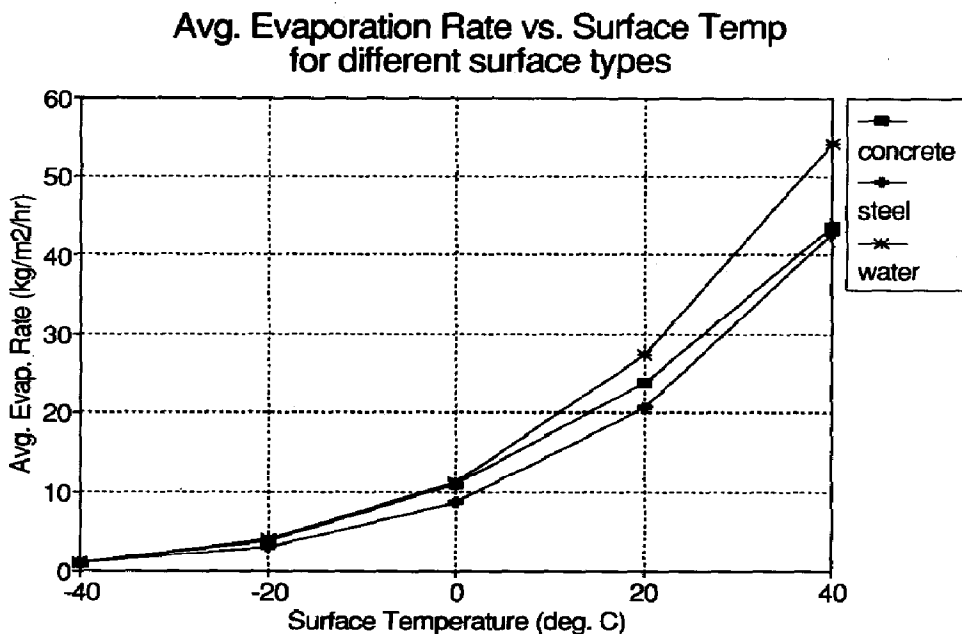


Fig. 9. Parametric validation test #1.

Avg. Evaporation Rate vs. Ambient Temp for different wind speeds

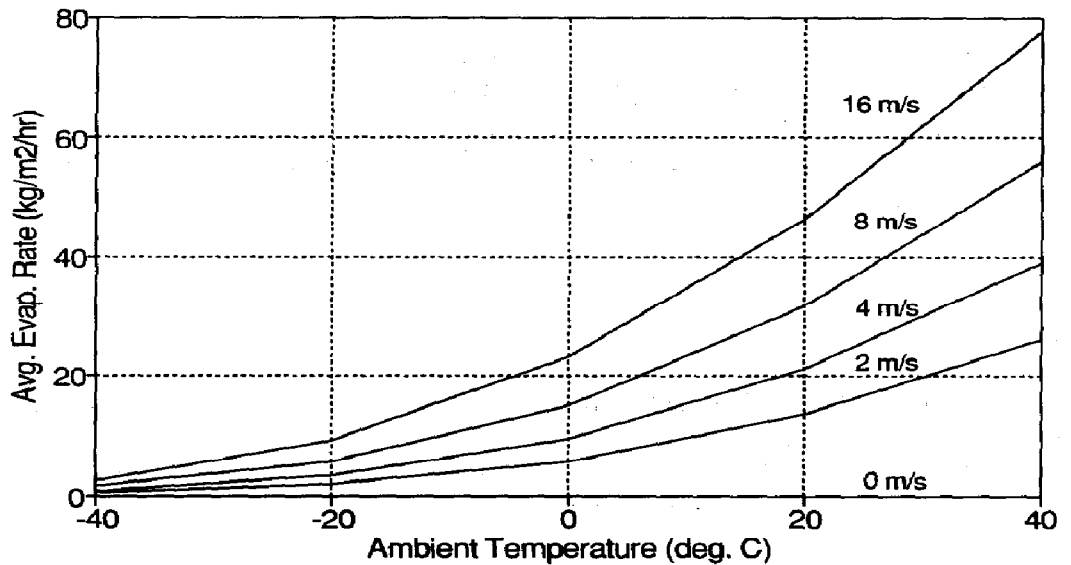


Fig. 10. Parametric validation test #2.

Avg. Evaporation Rate vs. Chemical NBP

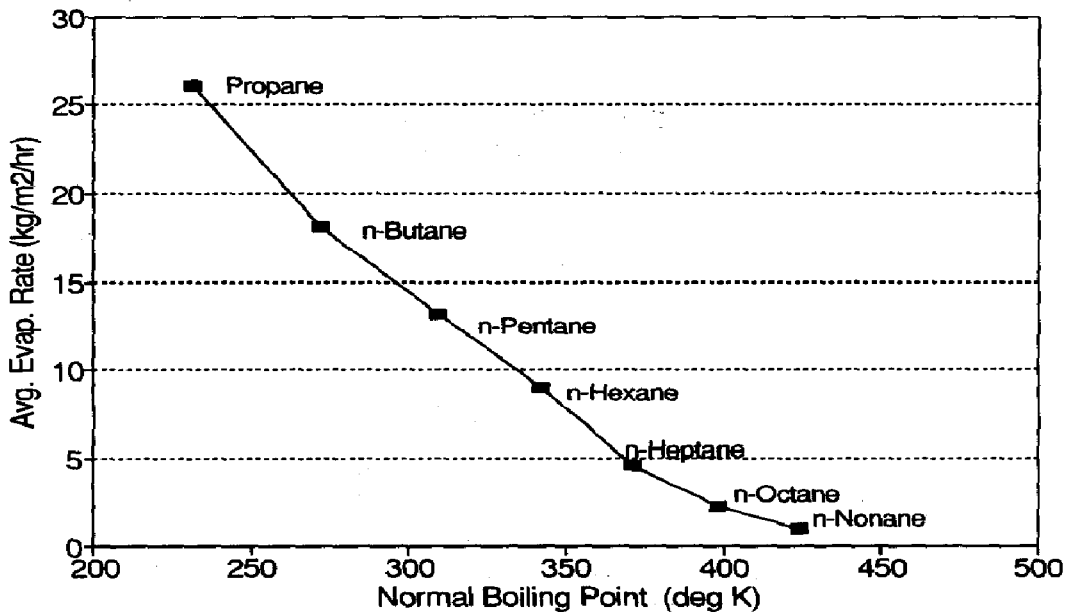


Fig. 11. Parametric validation test #3.

Time for Pool to Dry vs. Chemical for different spill sizes

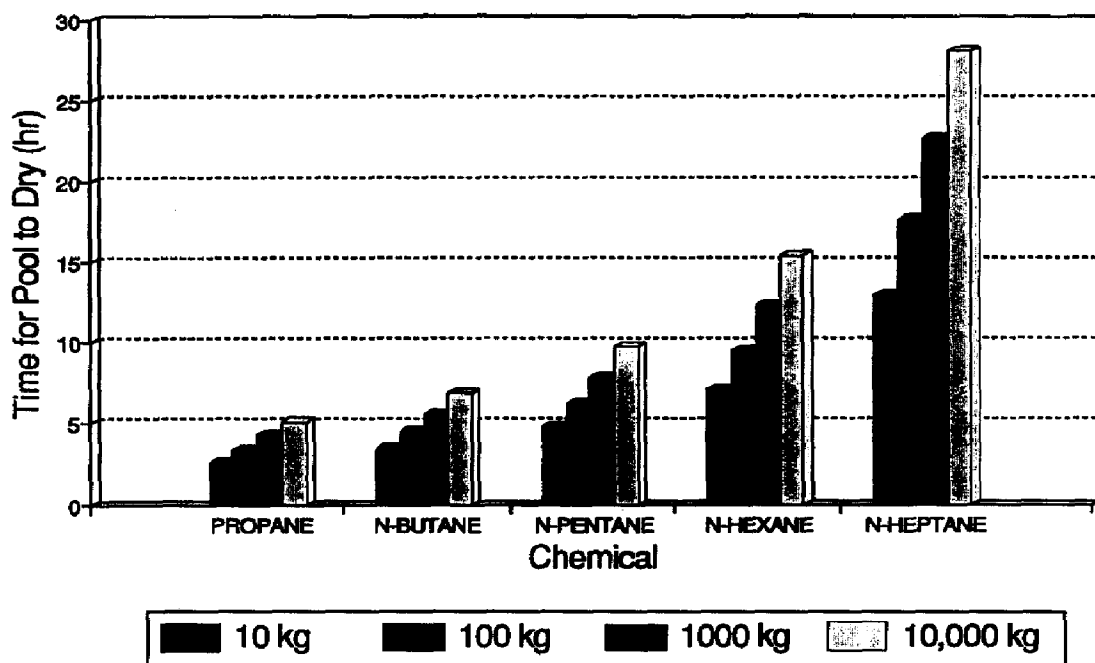


Fig. 12. Parametric validation test #4.

composition, initial liquid temperature, and spill size. In all cases the model responded as expected. Figures 9-12 show the results.

4.2. Tests against experimental results

Single component land spill evaporation rates were compared against experimental results reported by Kawamura, MacKay and Matsugu [7, 8]. LSM90 predicted the evaporation rates within 1-23% (with an average of 11%) of the experimental values. The experiments consisted of evaporating seven different chemicals from a flat circular pan and measuring their evaporation rate at steady state. LSM90 results were further analyzed by comparing its predicted values against two other models (the "direct evaporation" and "surface temperature" models) put forth in the published article. Figure 13 shows that LSM90 appears to outperform the other models in predicting the pool evaporation rate, especially at rates higher than 5 kg/m² h.

LSM90 was also tested against two sets of liquified natural gas (LNG) spills on water [9, 10]. Differences in the predicted vs. experimental evaporation values varied

Comparison of Models vs. the Kawamura & Mackay Experiments

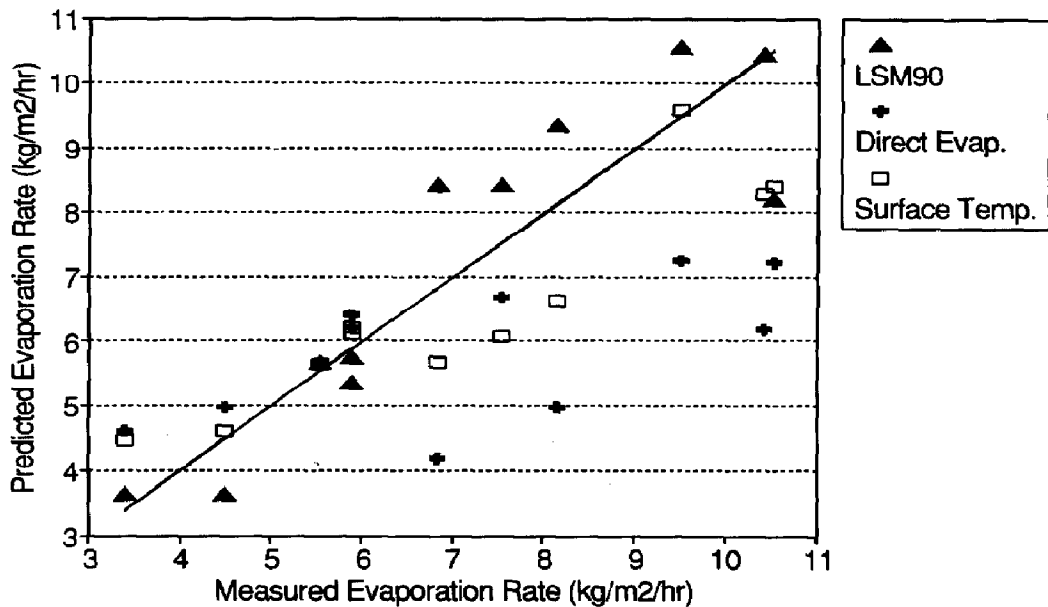


Fig. 13. Single component land spill validation.

Comparison of LSM90 vs. the Esso M.Bay and Burro Series Experiments

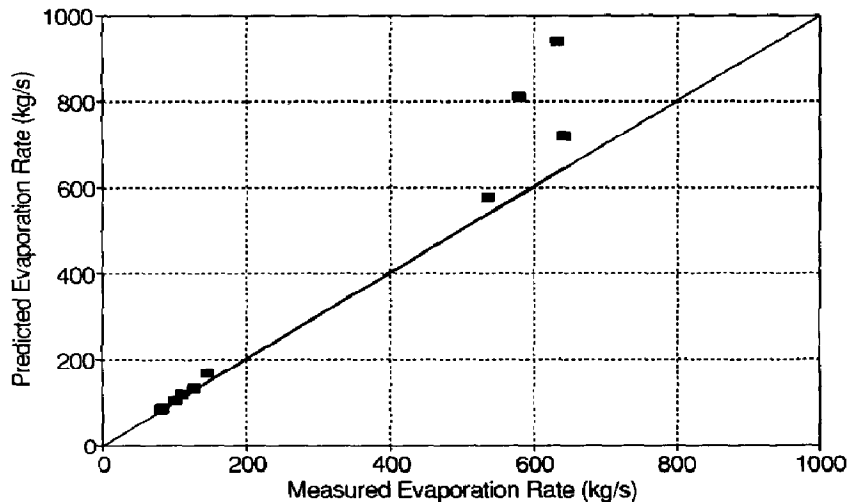


Fig. 14. Multicomponent spill on water validation.

from 1 to 48%, with 8 of the 10 cases coming within 14%. In addition, the average difference in the predicted vs. actual pool size was 12%. Figures 14 and 15 demonstrate LSM90's ability to predict open water LNG spill evaporation rates and pool sizes.

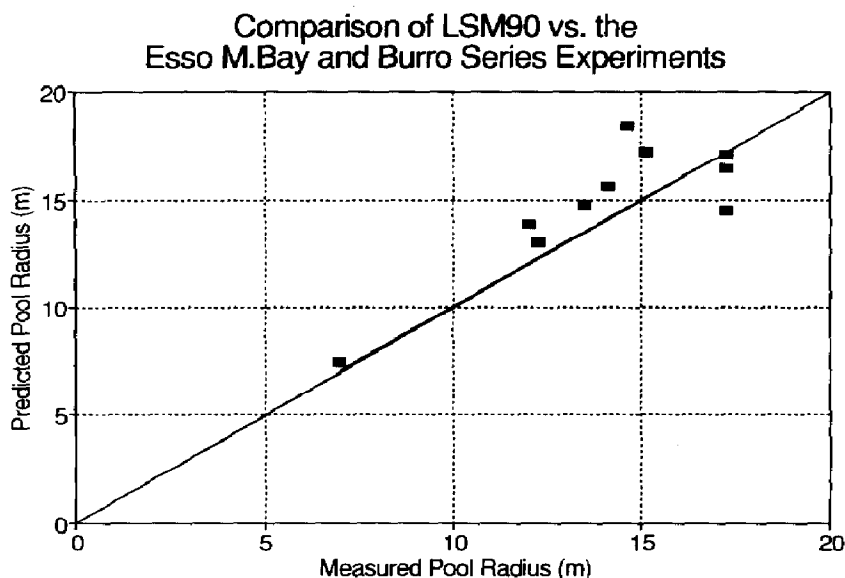


Fig. 15. Multicomponent spill on water pool size validation.

Nomenclature

A	pool area (m^2)
A_{hole}	area of hole (m^2)
A_i	contact area of segment i with the pool (m^2)
B	buoyancy factor (dimensionless)
cc	fraction of cloud cover
c_D	discharge coefficient (dimensionless)
C_p	liquid heat capacity (kcal/kg K)
C_{pm}	specific heat of air/vapor mixture (kcal/kg K)
dN_i/dt	rate of evaporation for component i (kg mol/s)
d_0	pool diameter (m)
f_{area}	area factor (dimensionless)
f_{aerosol}	fraction of unflashed liquid forming an aerosol
f_{flash}	fraction flashing
F_r	fluid reflectance (dimensionless)
g	acceleration due to gravity (m/s^2)
h	heat transfer coefficient (kcal/s_K m^2)
h_D	fraction of daylight in a day
h_{hole}	height of hole in storage tank (m)
h_{pool}	height of liquid in pool (m)
h_{tank}	height of liquid in storage tank (m)
i	section of contact area for heat transfer
j	component
k	thermal conductivity (kcal/s m K)

K_{gi}	mass transfer coefficient of component i at the air–pool interface (kg mol/m ² atm)
m	rate of mass spilling into the pool (kg/s)
m_{pool}	mass in pool (kg)
m_j	rate of component j evaporating (kg mol/s)
M	total number of components
M_{aerosol}	mass entrained as an aerosol (kg)
M_{flash}	mass flashed (kg)
$M_{\text{to pool}}$	liquid mass going to pool (kg)
M_{total}	total mass being released (kg)
N	total number of sections
N_i	number of moles of component i (kg mol)
N_T	total number of moles in the pool (kg mol)
p_i^s	saturation vapor pressure of component i (atm)
P_{amb}	ambient pressure (Pa)
Pr	Prandtl number of air
P_{sat}	saturation pressure (Pa)
P_{stag}	stagnation pressure (Pa)
P_{stor}	storage pressure (Pa)
q_{air}	heat transfer rate by air convection (kcal/s)
q_{dike}	heat transfer rate by dike conduction (kcal/s)
q_{evap}	rate of heat lost due to evaporation (kcal/s)
q_{ground}	heat transfer rate by ground conduction (kcal/s)
$q_{\text{mass_add}}$	heat transfer rate from mass added to the pools (kcal/s)
q_{rad}	heat transfer rate from long wave atmosphere radiation (kcal/s)
q_{sensible}	rate of heat gained or lost as the pool changes temperature (kcal/s)
q_{sun}	heat transfer rate from short wave sun radiation (kcal/s)
q_{tank}	heat transfer rate by tank conduction (kcal/s)
r_{new}	radius after expansion (m)
r_{old}	radius before expansion (m)
R	gas constant (0.08206 atm m ³ /kg mol K)
R_{evap}	specific evaporation rate (m/s)
R_{pool}	pool radius (m)
S_{noon}	noon time insolation on a clear day (2.39 kcal/m ² s)
Sc_i	Schmidt number of component i in the vapor phase
SR	sunrise, as a fraction of the day
t	time (s)
t_D	time of day, as a fraction of the day
t_i^*	time section i was first wetted (s)
T_{amb}	ambient temperature (K)
T_{dike}	dike temperature (K)
T_f	final pool temperature (K)
T_{ground}	ground temperature (K)
T_i	initial pool temperature (K)
T_{nbp}	liquid normal boiling point (K)

T_{pool}	liquid pool temperature (K)
T_{storage}	liquid storage temperature (K)
T_{tank}	tank temperature (K)
u_w	wind speed (m/s)
α	thermal diffusivity (m^2/s)
ΔR_v	change in net rate of volume entering or leaving the pool (m^3/s)
ΔV	change in pool volume (m^3)
ε	liquid emissivity ($\text{kcal}/\text{m}^2 \text{K}^4 \text{s}$)
ΔH_{vap}	latent heat of vaporization ($\text{kcal}/\text{kg mol}$)
$\Delta H_{\text{vap}j}$	heat of vaporization for component j ($\text{kcal}/\text{kg mol}$)
ρ	liquid density (kg/m^3)
ρ_m	density of the air/vapor mixture (kg/m^3)
σ	Stephen–Boltzman constant (dimensionless)

References

- [1] Workbook of Test Cases for Vapor Cloud Source Dispersion Models, Center for Chemical Process Safety of the AIChE, New York, 1989, p. 7.
- [2] Liquid RELEASE Final Report, Draft Copy, prepared for the AIChE Center for Chemical Process Safety, Creare Inc., 1988.
- [3] D.L. Ermak, User's Manual for SLAB: An Atmospheric Dispersion Model for Denser-than-Air Releases, Lawrence Livermore Laboratory, Livermore, CA, 1989.
- [4] P. Shaw and F. Briscoe, Evaporation from Spills of Hazardous Liquids on Land and Water, United Kingdom Atomic Energy Authority, 1978.
- [5] O.G. Sutton, Micrometeorology, McGraw-Hill, New York, 1953.
- [6] C.R. Wilke and C.Y. Lee, *Ind. Eng. Chem.*, 47 (1955) 1253.
- [7] P. Kawamura and D. MacKay, The evaporation of volatile liquids, *J. Hazardous Mater.*, 15 (1987) 343–364.
- [8] D. MacKay and R.S. Matsugu, Evaporation rates of liquid hydrocarbon spills on land and water, *Can. J. Chem. Eng.*, 51 (1973) 434–439.
- [9] G.F. Feldbaur et al., Spills of LNG on water — Vaporization and downwind drift of combustible mixtures, API Report EE61E-72, 1972.
- [10] Burro Series Data Report LLNL/NWC, 1980 LNG Spill Tests, Lawrence Livermore Laboratory, UCID 19075, Livermore, CA, 1982.